

Design of a Reconfigurable Intelligent Surface Algorithm Based on Multiple-Input Multiple-Output



Fuchun Jiang*, Weiming Lin, Hongyi Zhang, Xinhua Lin, Chenwei Feng

Fujian Key Laboratory of Optoelectronic Technology and Devices, Xiamen University of Technology, Xiamen 361024, China

Corresponding Author Email: jiangfuchun@xmut.edu.cn

<https://doi.org/10.18280/ts.390606>

ABSTRACT

Received: 30 August 2022

Accepted: 1 November 2022

Keywords:

reconfigurable intelligent surface (RIS), cell-free massive multiple input multiple output (MIMO), joint optimization algorithm, weighted sum rate (WSR)

Reconfigurable Intelligent Surface (RIS) can improve the security of the physical layer of wireless communication by adjusting the phase of the reflective unit. After analyzing the common theoretical models and potential problems, this study proposes an alternative iterative model based on multiple input multiple output (MIMO), and designs the transmitter, channel and receiver. In addition, passive beamforming precoding matrix of RIS was jointly optimized, and the Lagrangian dual relaxation (LDR) was adopted to decouple the nonconvex problem. After that, the active and passive beamforming matrices were subjected to iterative calculation, and the beamforming was optimized through cyclic programming at the base station (BS). In addition, the high convergence of the proposed algorithm was proved by MATLAB simulation. The results of simulation demonstrate that the joint precoding framework algorithm can maximize the weighted sum rate (WSR), which in turn demonstrates the feasibility of our method. Finally, the authors analyzed the strong applicability of the RIS technology in complex wireless networks with different volatility, revealing the possibility of future development.

1. INTRODUCTION

In recent years, China has made great progress in 5G wireless communication technology, and deployed more and more 5G base stations. Meanwhile, the 6G wireless network has piqued the interest of most operators, thanks to the technical advantages of 6G communication technology, such as ultra-high frequency spectrum, high energy efficiency, ultra-connection of ultra-dense users, and ultra-low latency [1]. The reasonable control of energy and power efficiency is crucial to the 6G wireless network. So far, researchers have studied the efficiency of various energy-intensive communication services, aiming to reasonably distribute the energy and power in the network.

Apart from energy efficiency, secure communication is also critical in the 6G wireless network. There are two types of secure communication technologies: the traditional encryption technology and security system, which encodes the transmitted information through software encryption, and the hardware data encryption on the physical layer, which realizes secure communication without incurring additional overhead during the protection of the safe key [2, 3]. One of such secure communication technologies is reconfigurable intelligent surface (RIS). The RIS improves the security of physical layer of wireless communication systems by adjusting the phase of the reflective unit. The introduction of RIS adds a special dimension to the design of wireless communication systems: interfering channels are designed to obtain a channel that can be controlled to a certain extent [2]. This extend depends on the integrated algorithm and the coverage density of the RIS system. Once the RIS is fully deployed in all directions of the transmitter and receiver, the wireless communication channel will be fully controllable [4].

Compared with traditional relays, the RIS is a passive, low-power device, which ensures that the transmission signal-to-noise ratio (SNR) in the channel is proportional to the square of the surface elements number of RIS [5]. Starting from this unique feature, a series of mathematical calculations can be carried out [4], allowing operators to change the deployment cost, and enabling scholars to realize deeper derivations. This is good news to the potential application of RIS research results.

The RIS is made of a new programmable two-dimensional (2D) metamaterial. The metamaterial is divided into several element units, which are combined into a surface structure. Each element unit needs to be adjusted to control the angle of reflection and intensity of incoming and outgoing electromagnetic waves, according to the mathematical and chemical components. The adjustment generally refers to changing the size of capacitance, resistance, and inductance. The RIS structure is illustrated in Figure 1. Following the one-to-one principle, each unit of each layer is connected to the corresponding controller [6].

In recent years, RIS has been widely studied in academia. The signal from the base station (BS) can reach the user equipment (UE) directly, or via RIS reflection. The phase of the N reflection elements of the RIS should be reasonably modulated, so that the RIS reflection signal is superimposed with the original signal at the spectrum sharer for the signal strength enhancement [7]. The common performance indices of wireless systems, such as SNR, secrecy rate (SR), transmission power, sum rate of multiple users (sum-rate), energy efficiency (EE), and physical layer security (PLS) [5] are generally assured by designing a joint optimization algorithm, which can start with the element phase of the RIS,

and also consider the joint optimization of the multi-antenna beamforming (BF, beamforming) vector of the BS.

Saad et al. [3, 8] explored the beam design problem of RIS-assisted multi-input single-output (MISO) system, and analyzed the robust beamforming design of the worst-case, in the presence of imperfect channel state information (CSI). Through transformation and approximation, the problem was transformed to a series of subproblems of the semi-definite program (SDP), followed by the reasoning about the system's data transfer rate and security. Huang et al. [9] calculated the symbol error probability (SEP), before analyzing the element number of the RIS per unit area, the effect of the corresponding phase on the SEP of system compilation, and the final asymptoticity. Lyu and Zhang [7] investigated the impact of RIS deployment on the downlink throughput in the MISO of the current wireless communication system, and proved that a denser deployment of RIS can greatly enhance the signal power at the cost of rising interference other than the preset interference.

Additionally, Saad et al. [3] pointed out that the per square meter capacity of the RIS surface area varies proportionally with the mean transmission power, rather than logarithmically as in the massive MIMO. Huang et al. [9] imagined the entire surface as a receiving antenna array to analyze the communication between a single antenna terminal and the RIS. In this case, the received post-filtering signal was matched. As long as the surface area is large enough, the channel

information could be represented by the inter-symbol interference channel constructed under the sinc function. Cui et al. [10] searched the optimal passive beamforming vector of RIS and the optimal active beamforming vector of BS to maximize the weighted sum of downlink rates, and these weights represent the priorities of mobile users. Furthermore, discrete RIS phase shift values were adopted to make the analysis simpler and more practical.

The RIS can intelligently modulate the information of the reflected signal via software control. In terms of security applications, the eavesdropping-proof design at the physical layer is a forward-looking consideration to improve the probability of secrecy. Wu and Zhang [6] summarized that the integration of the RIS in wireless communication systems intends to minimize the information leakage to the eavesdropper, and cut off the direct link between BS and eavesdropper by tuning the non-RIS reflected signal or the signal transmitted by the system. To maximize system security, Yang et al. [8] carried out the joint trajectory design and power control of unmanned aerial vehicles (UAVs), which properly adjusts the RIS reflection phase shift, and came up with a brand-new secure RIS UAV communication system. Considering discrete and continuous phase shifts, Chen et al. [11] designed an alternate optimization algorithm, and relied on the algorithm to optimize the transmit beamforming and RIS phase shift matrix. The proposed algorithm improves the safe data rate to a certain extent.

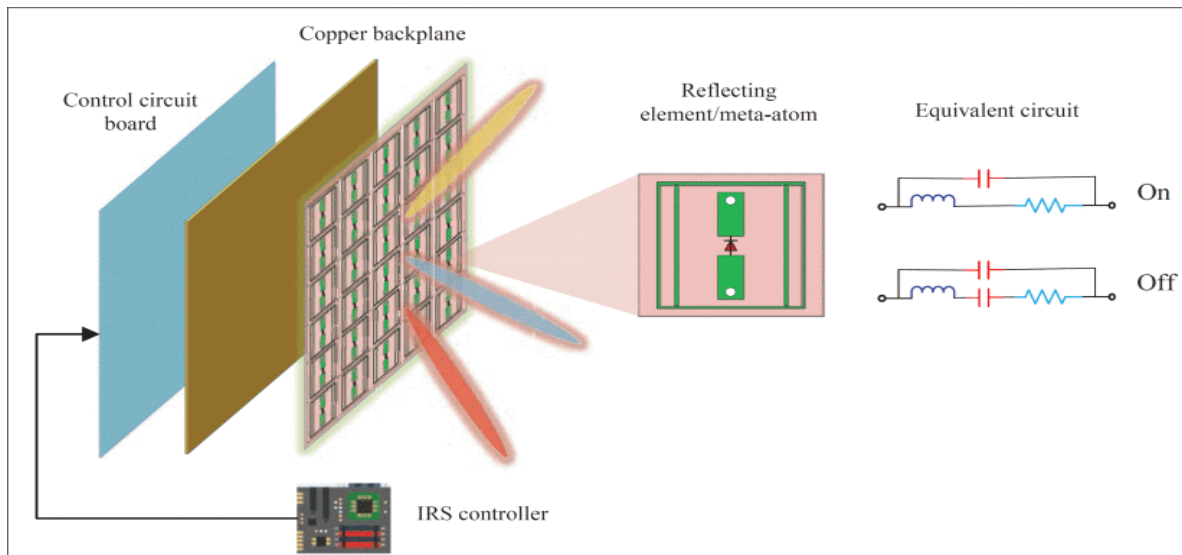


Figure 1. RIS structure

2. COMMON THEORETICAL MODELS AND POTENTIAL PROBLEMS

The RIS, which have an energy-efficient, high-gain, and low-cost meta-surface, can tune the phase shift of its elements with a lot of low-cost passive components, and reflect incident electromagnetic signals to any direction with high array gain [12]. Similar to the model shown in Figure 2, a common RIS includes a receiver, a random eavesdropper, a BS having N antennas, and an RIS having M phase shifters, whose phases are adjusted by the RIS controller.

When multiple signals arrive at the receiver simultaneously, the system will arrange them in an internal order called relative delay. If the difference between the relative delays is much less

than one bit time, then it can be assumed that they arrive at the receiver almost simultaneously. In this case, the multiple signals will not cause mutual interference between bits. Such an effective channel fading model is known as flat fading. Within each frequency band, the frequency response under this channel model is flat with little inter-bit interference. However, if the signals are superimposed, the influence of the relative delays will gradually increase, resulting in interference between bits. In this case, the frequency response of the channel is not flat in the frequency band. Such a fading model is known as the frequency selective fading model. Under this model, it is assumed that, after passing through the radio channel, the signal has a random amplitude, and its envelope obeys the Rayleigh distribution.

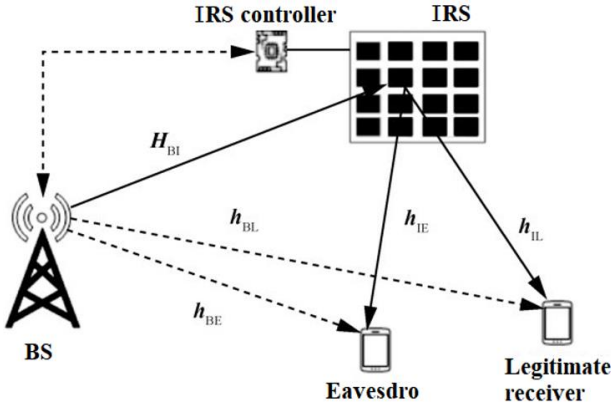


Figure 2. RIS-assisted downlink model of MISO

The quasi-static flat Rayleigh fading (QSRC) is a common channel model, where the multipath case does not cause inter-symbol interference and remains constant within each block. Therefore, this paper chooses the QSRC as the channel model. It is assumed that all CSI is known, and an eavesdropper is in the channel. Let $H_{BI} \in \mathbb{C}^{M \times N_t}$, $h_{BL} \in \mathbb{C}^{1 \times N_t}$, and $h_{IL} \in \mathbb{C}^{1 \times M}$ be the channel coefficient matrixs from BS to RIS, from BS to legitimate user, and from RIS to user, respectively. Drawing on idea of channel estimation, the signal received from legitimate receiver can be written as:

$$y_L = (h_{BL} + h_{IL}\Phi H_{BI})fx + n_L \quad (1)$$

where, $\Phi = \text{diag}(\beta_1 e^{j\theta_1}, \beta_2 e^{j\theta_2}, \dots, \beta_M e^{j\theta_M})$ is the coefficient matrix of RIS; $\beta_k \in [0, 1]$ and $\theta_k \in [0, 2\pi]$ are the amplitude and phase of the k -th unit of RIS.

Suppose RIS has a large power gain, and is expressed as $\beta_k=1$, $k=1, 2, \dots, M$ [5]; $f \in \mathbb{C}^{N_t \times 1}$ represents the integrated beamforming of the BS, where the power limit $\|f\| \leq \sqrt{P_{AP}}$, P_{AP} indicates the real-time maximum power that the BS can transmit; n_L represents other undesired noise near the receiver, which satisfies $n_L \sim \mathcal{CN}(0, \sigma_L^2)$.

In the same way, the signal received from the eavesdropper can be expressed as:

$$y_E = (h_{BE} + h_{IE}\Phi H_{BI})fx + n_E \quad (2)$$

where, $h_{IE} \in \mathbb{C}^{1 \times M}$ and $h_{BE} \in \mathbb{C}^{1 \times N_t}$, $h_{IE} \in \mathbb{C}^{1 \times M}$ are the matrices of channel coefficient from RIS to eavesdropper, and from BS to eavesdropper; n_E is other undesired noise near the eavesdropper, which satisfies $n_E \sim \mathcal{CN}(0, \sigma_E^2)$.

According to formulas (1) and (2), in the common sense of the RIS-assisted MISO system, the safe rate can be derived as:

$$R_{\text{sec}} = [R_L - R_E]^+ (\text{unit: bit}/(\text{s} \cdot \text{Hz})) \quad (3)$$

where, $[x]^+$ is mathematically the larger number between x and 0; R_L is the receiving rate of the legitimate receiver on the link:

$$R_L = \text{lb} \left(1 + \frac{|(h_{BL} + h_{IL}\Phi H_{BI})f|^2}{\sigma_L^2} \right) \quad (4)$$

The eavesdropper's receiving rate on the link should also be represented. Here, the eavesdropping rate R_E [5, 13] is defined as:

$$R_E = \text{lb} \left(1 + \frac{|(h_{BE} + h_{IE}\Phi H_{BI})f|^2}{\sigma_E^2} \right) \quad (5)$$

As shown in formula (3), in order to maximize R_{sec} , it is necessary to jointly design the key factor Φ of RIS and the vector f of BS, remove the mathematical symbol $[\cdot]^+$ in formula (3) through a certain transformation, and transform the formula as follows, using the incremental feature of $\text{lb}(\cdot)$:

$$\{f_{\text{opt}}, \Phi_{\text{opt}}\} = \arg \max_{f, \Phi} \frac{1 + \frac{|(h_{BL} + h_{IL}\Phi H_{BI})f|^2}{\sigma_L^2}}{1 + \frac{|(h_{BE} + h_{IE}\Phi H_{BI})f|^2}{\sigma_E^2}}$$

$$\text{s.t. } \|f\|^2 \leq P_{AP}$$

$$|\Phi_{i,i}| = 1, i \in \{1, 2, \dots, M\} \quad (6)$$

It can be observed from formula (6) that the constraints involve a series of non-convex problems, which limits the solution process. Meanwhile, there is a relationship between the variables in the objective function. The two constant optimization variables f and Φ are mutually coupled, making it possible to transform the objective function into a convex function step by step [5].

Restricted by the above conditions, the optimal solution of f and Φ in formula (6) cannot be directly obtained. Nevertheless, Constraint 1 in formula (6) only restricts f , and Constraint 2 only targets Φ .

So far, the algorithm using alternate iterative multiplication factors has already taken shape. The next goal is to design f and Φ separately until the objective function converges to a stable value [5].

3. MODELING AND JOINT OPTIMIZATION

The centralized massive MIMO technology is extensively adopted by the BSs in the current 5G cellular network communication system. The exiting research proves that the network capacity can be further expanded by increasing the density of BSs. But denser BS distribution increases the inter-cell interference, which seriously bottlenecks the continuous improvement of network capacity.

In 2017, wireless communication researchers came up with the cell-free massive MIMO technology, which achieves a larger network capacity than centralized massive MIMO. The excellent network capacity is realized by deploying distributed small BSs, and eliminating inter-cell interference through the cooperation between BSs. The integration of RIS in the cellular-free network (RIS-CF) provides a better way of the effective improvement of coverage and capacity at low cost, without consuming much power, for the future wireless systems. This paper randomly distributes multiple access points (APs), and constructs a centrally distributed backhaul link model to transmit data to the central processing unit (CPU) while ensuring that the frequency consistency between all multi-frequency signals. At the same time, the received signal of user was enhanced by programming the reflection coefficient of the RIS. Figure 3 presents the structure of the cellular-free network.

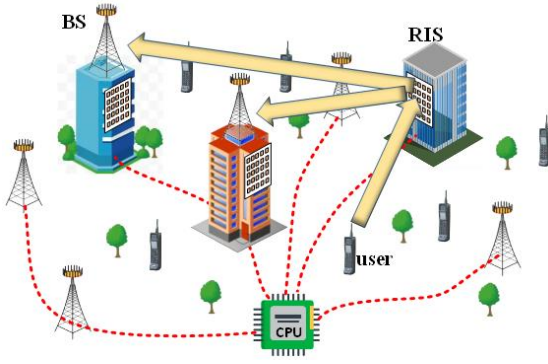


Figure 3. Structure of cellular-free network

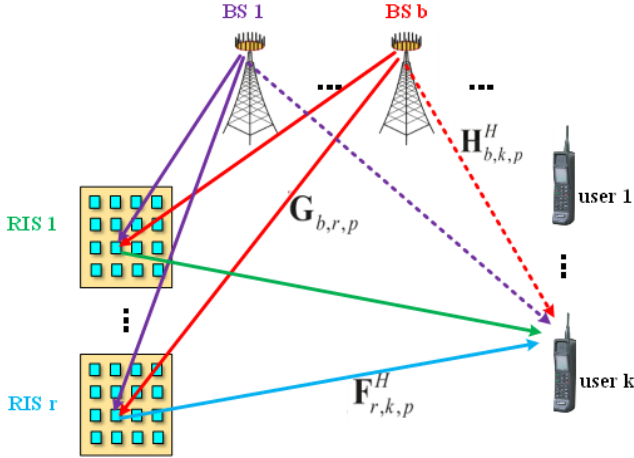


Figure 4. Downlink channel of RIS-CF system

The cellular-free massive MIMO network can shorten the distance between the user and the BS, and obtain a spatially distributed absolute gain. It can also greatly reduce the path loss in the effective transmission channel, and utilize a massive number of APs to ensure favorable propagation to numerous users. In this way, the resource waste is avoided, and the interference between multiple bits is reduced.

The prototype of the system is a distributed antenna system (DAS), which can be compared to identify the origin of RIS-CF. Figure 4 shows the new network system proposed by the authors: The proposed system contains BSs, R RISs, and K multi-antenna users. The number of antennas of the b -th BS, the number of antennas of the k -th user, and the number of elements of the r -th RIS are denoted by M_b , U_k and N_r , respectively. For simplicity, M_b , U_k and N_r are written simply as M , U , and N , respectively.

Considering the need for multi-carrier transmission, it is further assumed that there are P subcarriers. Then, the number of RIS elements, RISs, BSs, subcarriers, and users is denoted by $\mathcal{N} = \{1, \dots, N\}$, $\mathcal{R} = \{1, \dots, R\}$, $\mathcal{B} = \{1, \dots, B\}$, $\mathcal{P} = \{1, \dots, P\}$, and $\mathcal{K} = \{1, \dots, K\}$, respectively.

3.1 Transmitter design

In the cellular-free massive MIMO network, all BSs must be synchronized and independent to provide better service to all users through an integrated channel.

Assume $s_p \triangleq [s_{p,1}, \dots, s_{p,K}]^T \in \mathbb{C}^K$, in which $s_{p,k}$ represents the bit information sent on the p -th subcarrier for the k -th user. Suppose the power of transmitted signals are same, e.g., $\mathbb{E}\{s_p s_p^H\} = I_K, \forall p \in \mathcal{P}$. In the transmission model of downlink,

the frequency domain symbol $s_{p,k}$ is first decoded on the b -th BS with the precoding vector $w_{b,p,k} \in \mathbb{C}^M$.

Therefore, at the b -th BS on the p -th subcarrier, the precoding $x_{b,p}$ can be expressed as:

$$x_{b,p} = \sum_{k=1}^K w_{b,p,k} s_{p,k} \quad (7)$$

At the b -th BS on the p -th subcarrier, the frequency domain symbol $\{x_{b,p}\}_{p=1}^P$ can be transformed into the time domain by inverse discrete Fourier transform (IDFT). After being added a cyclic prefix (CP), the signal is up-transformed into the radio frequency (RF) domain through the M radio frequency chains.

3.2 Channel design

As shown in the RIS-CF system, the R RISs support directional reflection. In the RIS-CF system network, the channel between each pair of user and BS is roughly composed of two parts: R BS-RIS user links and a freely distributed user-user link. Each BS-RIS user link consist of an RIS-user link and a BS-RIS link. Before be transmitted to the user, the RIS signal are modeled by multiplying the incident wave with a phase shift matrix. So, the channel $h_{b,k,p}^H \in \mathbb{C}^{U \times M}$ on the p -th subcarrier, from the b -th BS to the k -th user, can be equivalently expressed as:

$$h_{b,k,p}^H = \underbrace{H_{b,k,p}^H}_{\text{BS-user link}} + \sum_{r=1}^R \underbrace{F_{r,k,p}^H \Theta_r^H G_{b,r,p}}_{\text{BS-RIS-user link}} \quad (8)$$

in which, $H_{b,k,p}^H \in \mathbb{C}^{U \times M}$, $F_{r,k,p}^H \in \mathbb{C}^{U \times N}$, and $G_{b,r,p} \in \mathbb{C}^{N \times M}$ are the frequency domain channel of subcarrier p from b -th BS to k -th user, from r -th RIS to k -th user, and from b -th BS to r -th RIS; $\Theta_r \in \mathbb{C}^{N \times N}$ is the phase shift matrix of r -th RIS:

$$\Theta_r \triangleq \text{diag}(\theta_{r,1}, \dots, \theta_{r,N}), \forall r \in \mathcal{R} \quad (9)$$

where, $\theta_{r,n} \in \mathcal{F}$ and \mathcal{F} is a valid set of reflection coefficients (RCs) of RIS. For a generalized model, this paper assumes that \mathcal{F} is a system scenario based on the ideal RIS: both the phase and amplitude associated with the element $\theta_{r,n}$ of RIS can be controlled continuously and independently:

$$\mathcal{F} \triangleq \{\theta_{r,n} | |\theta_{r,n}| \leq 1\}, \forall r \in \mathcal{R}, \forall n \in \mathcal{N} \quad (10)$$

3.3 Receiver design

Assume the received signal by the user pass through the channel $h_{b,k,p}^H$. The signal in time domain is first transform to the baseband by frequency transform, followed by CP removal and discrete Fourier transform (DFT). The original signal can be restore with the final frequency domain symbol. Let $y_{b,k,p} \in \mathbb{C}^U$ denote the baseband signal in frequency domain, which transmit from b -th BS to k -th user via subcarrier p . Then, $y_{b,k,p}$ can be derived according from the channel model above. Since B BSs serve K users simultaneously, this paper adopts the matrix-based idea, and superimposes the signals received at user k with the transmitted signals from B BSs. Let $y_{k,p} \in$

\mathbb{C}^U denote the received signal of k-th user on subcarrier p. With the additive white Gaussian noise (AWGN) at the receiver, $y_{k,p}$ can be written as formula (11):

$$\begin{aligned} y_{b,k,p} &= \mathbf{h}_{b,k,p}^H \mathbf{x}_{b,p} \\ &= \left(\mathbf{H}_{b,k,p}^H + \sum_{r=1}^R \mathbf{F}_{r,k,p}^H \Theta_r^H \mathbf{G}_{b,r,p} \right) \sum_{j=1}^K \mathbf{w}_{b,p,j} s_{p,j} \end{aligned} \quad (11)$$

$$\begin{aligned} y_{k,p} &= \sum_{b=1}^B y_{b,k,p} + z_{k,p} = \sum_{b=1}^B \sum_{j=1}^K (\mathbf{H}_{b,k,p}^H + \sum_{r=1}^R \mathbf{F}_{r,k,p}^H \Theta_r^H \mathbf{G}_{b,r,p}) \mathbf{w}_{b,p,j} s_{p,j} + z_{k,p} \\ &= \underbrace{\sum_{b=1}^B (\mathbf{H}_{b,k,p}^H + \sum_{r=1}^R \mathbf{F}_{r,k,p}^H \Theta_r^H \mathbf{G}_{b,r,p}) \mathbf{w}_{b,p,k} s_{p,k}}_{\text{Desired signal to user k}} \\ &\quad + \underbrace{\sum_{b=1}^B \sum_{j=1, j \neq k}^K (\mathbf{H}_{b,k,p}^H + \sum_{r=1}^R \mathbf{F}_{r,k,p}^H \Theta_r^H \mathbf{G}_{b,r,p}) \mathbf{w}_{b,p,j} s_{p,j}}_{\text{Interference from other users}} + z_{k,p} \end{aligned} \quad (12)$$

3.4 Scheme generation

Based on the above system model, the weighted sum rate (WSR) of the cellular-free massive MIMO network is maximized, under the constraints of transmission power in BSs and RC-constrained RISs.

First, the received signal $y_{b,k,p}$ in formula (12) can be simplified as:

$$\begin{aligned} y_{k,p} &\stackrel{(a)}{=} \sum_{b=1}^B \sum_{j=1}^K (\mathbf{H}_{b,k,p}^H + \mathbf{F}_{k,p}^H \Theta^H \mathbf{G}_{b,p}) \mathbf{w}_{b,p,j} s_{p,j} \\ &\quad + z_{k,p} \stackrel{(b)}{=} \sum_{b=1}^B \sum_{j=1}^K \mathbf{h}_{b,k,p}^H \mathbf{w}_{b,p,j} s_{p,j} \quad (13) \\ &\quad + z_{k,p} \stackrel{(c)}{=} \sum_{j=1}^K \mathbf{h}_{k,p}^H \mathbf{w}_{p,j} s_{p,j} + z_{k,p} \end{aligned}$$

In (a), Θ can be defined as:

$$\begin{aligned} \Theta &= \text{diag}(\Theta_1, \dots, \Theta_R), \mathbf{F}_{k,p} = [\mathbf{F}_{1,k,p}^T, \dots, \mathbf{F}_{R,k,p}^T]^T, \mathbf{G}_{b,p} \\ &= [\mathbf{G}_{b,1,p}^T, \dots, \mathbf{G}_{b,R,p}^T]^T \end{aligned}$$

(b) mainly comes from formula (11);

In (c), $\mathbf{h}_{k,p}$ can be defined as:

$$\mathbf{h}_{k,p} = [\mathbf{h}_{1,k,p}^T, \dots, \mathbf{h}_{B,k,p}^T]^T, \mathbf{w}_{p,k} = [\mathbf{w}_{1,p,k}^T, \dots, \mathbf{w}_{B,p,k}^T]^T$$

Then, for the k-th user on subcarrier p, the transmission symbol $s_{p,k}$ SINR can be calculated by:

$$\begin{aligned} \gamma_{k,p} &= \mathbf{w}_{p,k}^H \mathbf{h}_{k,p} \left(\sum_{j=1, j \neq k}^K \mathbf{h}_{k,p}^H \mathbf{w}_{p,j} (\mathbf{h}_{k,p}^H \mathbf{w}_{p,j})^H \right. \\ &\quad \left. + \Xi_{k,p} \right)^{-1} \mathbf{h}_{k,p}^H \mathbf{w}_{p,k} \end{aligned} \quad (14)$$

For all K users, the WSR R_{sum} can be derived by:

$$R_{\text{sum}} = \sum_{k=1}^K \sum_{p=1}^P \eta_k \log_2 (1 + \gamma_{k,p}) \quad (15)$$

Note that the first term on the right side of formula (11) represents the expected signal of user k in effective transmission. Since there are a total of P available subcarriers, this paper makes the seemingly complex expression of the second term as the interference signal. The corresponding signal received by the user is denoted by $\{y_{k,p}\}_{p=1}^P$. Then, we have:

where, $\eta_k \in \mathbb{R}^+$ is the weight of k-th user; $R_{k,p}$ is the rate of k-th user on subcarrier p.

Finally, the problem of WSR maximization can be initially expressed as

$$\begin{aligned} \mathcal{P}^\circ: \max_{\Theta, \mathbf{W}} R_{\text{sum}}(\Theta, \mathbf{W}) \\ = \sum_{k=1}^K \sum_{p=1}^P \eta_k \log_2 (1 + \gamma_{k,p}) \end{aligned} \quad (16a)$$

$$\text{s.t. } C_1: \sum_{k=1}^K \sum_{p=1}^P \|\mathbf{w}_{b,p,k}\|^2 \leq P_{b,\max}, \forall b \in \mathcal{B} \quad (16b)$$

$$C_2: \theta_{r,n} \in \mathcal{F}, \forall r \in \mathcal{R}, \forall n \in \mathcal{N} \quad (16c)$$

where, $P_{b,\max}$ is the maximum transmission power of b-th BS. For convenience, \mathbf{W} can be defined as:

$$\mathbf{W} = [\mathbf{w}_{1,1}^T, \mathbf{w}_{1,2}^T, \dots, \mathbf{w}_{1,K}^T, \mathbf{w}_{2,1}^T, \mathbf{w}_{2,2}^T, \dots, \mathbf{w}_{P,K}^T]^T \quad (17)$$

It is very difficult to jointly optimize the non-convex objective function (16a), the precoding vector \mathbf{W} and the phase shift matrix Θ . Inspired by distribution programming (DP), the joint precoding framework algorithm—Lagrangian dual relaxation (LDR) was employed to find the solution to the problem \mathcal{P}° .

3.5 Algorithm optimization

The signal received by a single user will only be interfered by itself, rather than by other users. To facilitate the measurement and evaluation of the data throughput of system users, the problem was transformed into a joint optimization problem of how to design the beamforming vectors at the active and reflector ends. The problem cannot be solved directly, for the relative constraints of the objective function are not convex. Therefore, the non-convex problem was decomposed into multiple sub-problems for iterative joint solution.

It is assumed that the CSI in the time unit is known. To solve the logarithmic complexity and the WSR maximization, the LDR was adopted to apply logarithmic decoupling. This paper proposes a passive precoding and joint active framework to iteratively optimize these variables:

Inputs: $\mathbf{H}_{b,k,p}$, $\mathbf{G}_{b,r,p}$, and $\mathbf{F}_{r,k,p}$ of all channels, where $p \in \mathcal{P}$, $k \in \mathcal{K}$, and $\forall b \in \mathcal{B}$.

Outputs: optimized passive precoding matrix Θ ; optimized active precoding vector \mathbf{W} ; WSR R_{sum} .

Initializing W , and Θ ;

When R_{sum} does not converge, kicking off the following loop: update ρ ; update ξ ; update W ; update ϖ ; update Θ ; return W^{opt} , Θ^{opt} , and R_{sum} .

In the framework, these five variables ρ , ϖ , Θ , ξ , and W are updated iteratively until the objective function converges. The analytical solutions of ξ^{opt} , W^{opt} , ϖ^{opt} , and Θ^{opt} are obtained through further Lagrangian operations [14].

(1) Objective function

The auxiliary variable $\rho \in \mathbb{R}^{PK}$ was introduced, with $\rho = [\rho_{1,1}, \rho_{1,2}, \dots, \rho_{1,K}, \rho_{2,1}, \rho_{2,2}, \dots, \rho_{P,K}]^T$. Then, problem \mathcal{P}^o in formula (16) can be converted into:

$$\begin{aligned} \bar{\mathcal{P}}: \max_{\Theta, W, \rho} & f(\Theta, W, \rho) \\ \text{s.t. } C_1: & \sum_{k=1}^K \sum_{p=1}^P \|w_{b,p,k}\|^2 \leq P_{b,m}, \forall b \in \mathcal{B}, \\ C_2: & \theta_{r,n} \in \mathcal{F}, \forall r \in \mathcal{R}, \forall n \in \mathcal{N}, \end{aligned} \quad (18)$$

Then, the new objective function can be written as (Θ, W, ρ) :

$$\begin{aligned} f(\Theta, W, \rho) = & \sum_{k=1}^K \sum_{p=1}^P \eta_k \ln(1 + \rho_{k,p}) \\ & - \sum_{k=1}^K \sum_{p=1}^P \eta_k \rho_{k,p} \\ & + \sum_{k=1}^K \sum_{p=1}^P \eta_k (1 + \rho_{k,p}) f_{k,p}(\Theta, W) \end{aligned} \quad (19)$$

where, function $f_{k,p}(\Theta, W)$ is defined as:

$$\begin{aligned} f_{k,p}(\Theta, W) = & w_{p,k}^H h_{k,p} \left(\sum_{j=1}^K h_{k,p}^H w_{p,j} (h_{k,p}^H w_{p,j})^H \right. \\ & \left. + \Xi_{k,p} \right)^{-1} h_{k,p}^H w_{p,k} \end{aligned} \quad (20)$$

(2) Iteration of ρ^{opt}

Whereas (Θ^*, W^*) is known, for $\forall p \in \mathcal{P}$, and $\forall k \in \mathcal{K}$, the optimal ρ^{opt} of formula (20) got by solving $\partial f / \partial \rho_{k,p} = 0$. The solution can be expressed as:

$$\rho_{k,p}^{opt} = \gamma_{k,p}^*, \quad \forall p \in \mathcal{P}, \forall k \in \mathcal{K}. \quad (21)$$

Substituting $\rho_{k,p}^{opt}$ in formula (21) into f in formula (19), only the last term of formula (19) is related to variables Θ and W . Thus, the problem $\bar{\mathcal{P}}$ in formula (18) can be solved.

3.6 Simulation and discussion

This paper intensively adopts the LDR, along with repeated multi-dimensional complex quadratic transforms, to solve the original problem as multiple sub-problems. To verify the stability of the joint optimization algorithm framework proposed in this work, Matlab simulation was conducted to demonstrate the powerful performance of the proposed cellular-free massive MIMO network.

(1) WSR at different distances L

Referring to the potential deployment schemes of cellular-free networks, the simulation scenario for the cellular-free

MIMO network was designed by superimposing the dual time scale scheme onto the potential schemes. Suppose there are four users in a circle with the center of $(L, 0)$ and a radius of 1m. These users were randomly distributed, and height of them was set to 1.5m. Then, the WSR at different distances L can be obtained (Figure 5).

The following can be seen from Figure 5:

1) For the ideal RIS, the WSR can be maximized by the joint precoding framework algorithm.

2) When all direct links between users and BSs are blocked ($H=0$), the joint precoding framework algorithm can also maximize the WSR.

3) With the randomly setting of all phase shifts of RIS elements, the WSR can maximized by the joint precoding framework algorithm, based only on the composite channels at BSs.

4) For the RIS-free traditional cellular-free network, the WSR maximization effect is weakened, when the multi-user precoding method is implemented at BSs, based on the CSI of the BS user channels.

In general, it can be concluded that:

1) For the schemes with RIS, two obvious peaks can be seen at $L=60\text{m}$ and $L=100\text{m}$. This suggests that the WSR increases as the user approaches one of the two RIS, as the user may receive a strong signal reflected from the RIS. For the schemes without RIS, these two peaks do not appear. It can be concluded that deploying RIS in the network can greatly expand the network capacity, thereby extending the signal coverage.

2) Compared with the RIS-free schemes, the random phase shift leads to a very limited performance gain. The reason is as follows: if the RISs do not have passive beamforming, the signal arriving at the RISs cannot be directed to the user accurately, and that is the reason why passive precoding is necessary.

3) Compared with the ideal RIS scheme, the dual time scale scheme has a mean performance loss of about 10%. The possible reasons are: for the ideal RIS scheme, all RIS auxiliary channels are acquires and utilizes for joint precoding design, but for the dual time scale scheme, only the RIS auxiliary channels that match the user RIS pair are acquires and utilizes.

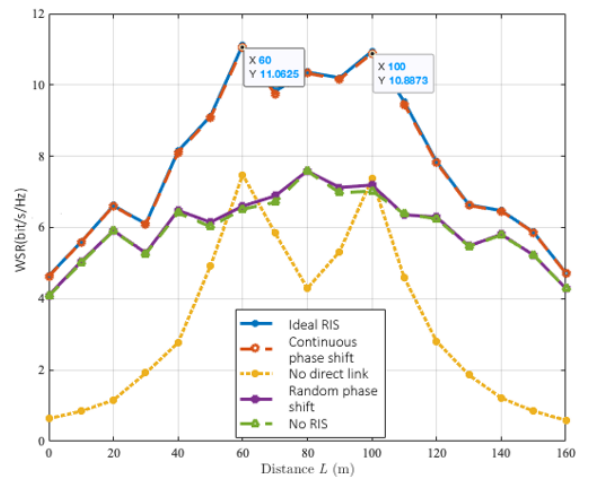


Figure 5. WSR at different distances L

(2) Framework Convergence

To demonstrate its convergence, our algorithm was run once after initialization, and the WSR results were compared

with the number of iterations in Figure 6, with the distance L fixed at 65m. Continuous phase shift, 1 bit phase shift, and 2 bit phase shift were added to represent different frequency domain cases, and evaluate the convergence in the case of non-ideal RIS phase shift.

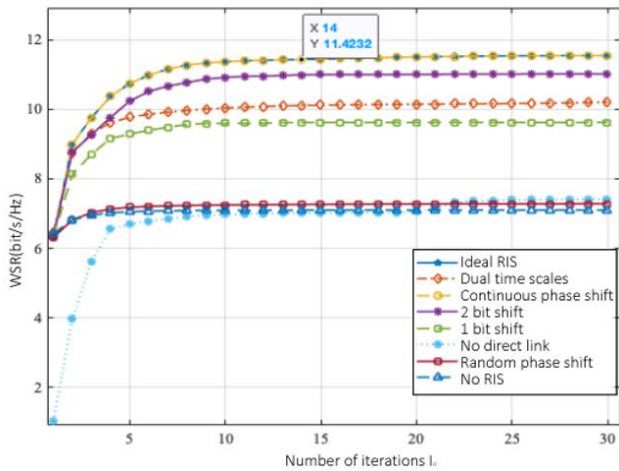


Figure 6. WSR at different CSI error parameters

The following can be seen from Figure 6:

1) When the convergence error does not exceed 1%, the joint precoding framework under RIS converges generally within 14 iterations. It can be seen that the ideal RIS scheme, dual time scale scheme, continuous phase shift scheme and no direct link scheme, all of which involve certain RIS, can converge in or around 14 iterations. By contrast, the discrete phase-shift scheme converges within 10 iterations, which indicates a certain error rate.

2) Since traditional cell-free networks without random phase shift scheme and RIS do not have the necessity to deal with RIS precoding, in these cases, no more than 5 iterations are needed for the WSR convergence.

3) The continuous phase shift curves and ideal RIS are very close. The reason might be that the magnitude of most optimized RIS elements is equal to 1 for the ideal RIS. Therefore, the amplitude limitation can be relaxed to optimize the precoding to the ideal RIS, for the precoding design of RIS with uncontrollable amplitude.

(3) Robustness Analysis

In the cellular-free massive MIMO network, estimation of channel is difficult due to the high-dimensionality of the channels. Thence, the authors decided to analyze the robustness of the joint precoding scheme to CSI errors.

In realistic, the actual estimated imperfect channel \hat{h} can be modeled as:

$$\hat{h} = h + e, \quad (22)$$

i.e. $e \sim \mathcal{CN}(0, \sigma_e^2), \sigma_e^2 \triangleq \delta|h|^2$.

where, e is the estimation error of Gaussian distribution and zero mean; h is the real channel; σ_e^2 is variance; δ is the error power. σ_e^2 is proportional to channel gain $\delta|h|^2$, reflecting the degree of CSI error.

As shown in Figure 7, the performance loss increases with time, especially for the ideal RIS vs. the perfect CSI with no error (i.e., $\delta = 0$). When the error power is 10% of the channel gain (i.e., $\delta = 0.1$), the system performance loses 5%; when $\delta = 0.3$, it loses 20%. It can be concluded that the joint precoding scheme is highly robust against CSI errors.

Therefore, it can be concluded that the joint precoding scheme has strong robustness to CSI errors.

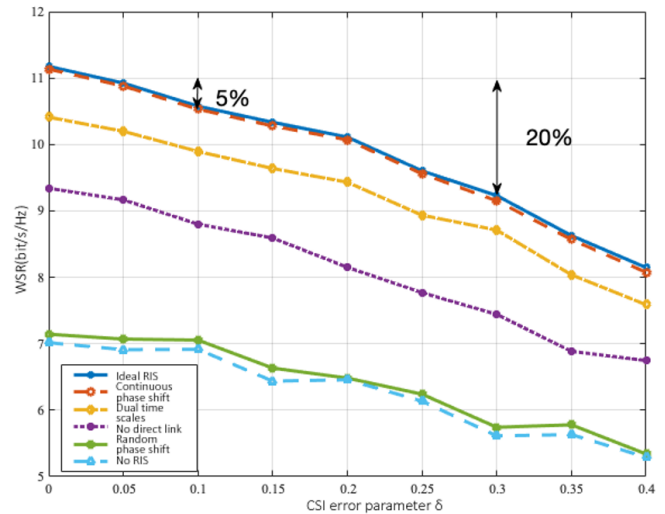


Figure 7. Robustness of joint precoding under CSI errors

4. CONCLUSIONS

This paper devises an RIS-assisted cellular-free network, evaluates the WSR and other properties of the network, and designs a joint precoding scheme, which optimizes the network capacity by maximizing the WSR. The results of simulation show that, with the help of energy-efficient and low-cost RIS, the proposed RIS-assisted cellular-free massive MIMO network can achieve higher capacity than traditional cellular-free networks, reduce transmit power [15], improve the transmission efficiency and reliability [16], and expand the coverage of wireless transmission [17-27].

RIS-assisted communication is an emerging research topic. In recent years, many scholars have expressed the hope of fundamentally changing the future wireless network architecture by integrating RIS, turning the traditional active component-only architecture into a new hybrid architecture. The transform of network architecture would significantly broaden the availability of energy in the future [6]. RIS is bound to become a promising key technology for 6G wireless communication.

ACKNOWLEDGEMENT

This project was supported by the Natural Science Foundation of Fujian Province of China (Grant No.: 2022J011271).

REFERENCES

- [1] Huang, C., Hu, S., Alexandropoulos, G.C., Zappone, A., Yuen, C., Zhang, R., Debbah, M. (2020). Holographic MIMO surfaces for 6G wireless networks: Opportunities, challenges, and trends. *IEEE Wireless Communications*, 27(5): 118-125. <https://doi.org/10.1109/MWC.001.1900534>
- [2] Wu, Y., Wen, C.K., Chen, W., Jin, S., Schober, R., Caire, G. (2019). Data-aided secure massive MIMO

- transmission under the pilot contamination attack. *IEEE Transactions on Communications*, 67(7): 4765-4781. <https://doi.org/10.1109/TCOMM.2019.2907943>
- [3] Saad, W., Bennis, M., Chen, M. (2019). A vision of 6G wireless systems: Applications, trends, technologies, and open research problems. *IEEE Network*, 34(3): 134-142. <https://doi.org/10.1109/MNET.001.1900287>
- [4] Yao, J.W., Wang, N. (2020). Intelligent Reflector - Promising 6G technology. *Telecommunications Information*, 4(7): 8-13.
- [5] Jing, X.R., Song, Z.Y., Gao, W. (2022). Design scheme of physical layer security for intelligent reflecting surface-assisted MISO communication system. *Journal on Communications*, 43(1): 117-126.
- [6] Wu, Q., Zhang, R. (2019). Towards smart and reconfigurable environment: Intelligent reflecting surface aided wireless network. *IEEE Communications Magazine*, 58(1): 106-112. <https://doi.org/10.1109/MCOM.001.1900107>
- [7] Lyu, J., Zhang, R. (2021). Hybrid active/passive wireless network aided by intelligent reflecting surface: System modeling and performance analysis. *IEEE Transactions on Wireless Communications*, 20(11): 7196-7212. <https://doi.org/10.1109/TWC.2021.3081447>
- [8] Yang, G., Xu, X., Liang, Y. C. (2020). Intelligent reflecting surface assisted non-orthogonal multiple access. In 2020 IEEE Wireless Communications and Networking Conference (WCNC), 1-6. <https://doi.org/10.1109/WCNC45663.2020.9120476>
- [9] Huang, C., Zappone, A., Alexandropoulos, G.C., Debbah, M., Yuen, C. (2019). Reconfigurable intelligent surfaces for energy efficiency in wireless communication. *IEEE Transactions on Wireless Communications*, 18(8): 4157-4170. <https://doi.org/10.1109/TWC.2019.2922609>
- [10] Cui, M., Zhang, G., Zhang, R. (2019). Secure wireless communication via intelligent reflecting surface. *IEEE Wireless Communications Letters*, 8(5): 1410-1414. <https://doi.org/10.1109/LWC.2019.2919685>
- [11] Chen, J., Liang, Y.C., Pei, Y., Guo, H. (2019). Intelligent reflecting surface: A programmable wireless environment for physical layer security. *IEEE Access*, 7: 82599-82612. <https://doi.org/10.1109/ACCESS.2019.2924034>
- [12] Basar, E., Di Renzo, M., De Rosny, J., Debbah, M., Alouini, M.S., Zhang, R. (2019). Wireless communications through reconfigurable intelligent surfaces. *IEEE Access*, 7: 116753-116773. <https://doi.org/10.1109/ACCESS.2019.2935192>
- [13] Cui, M., Zhang, G., Zhang, R. (2019). Secure wireless communication via intelligent reflecting surface. *IEEE Wireless Communications Letters*, 8(5): 1410-1414. <https://doi.org/10.1109/LWC.2019.2919685>
- [14] Zhang, Z., Dai, L. (2021). A joint precoding framework for wideband reconfigurable intelligent surface-aided cell-free network. *IEEE Transactions on Signal Processing*, 69: 4085-4101. <https://doi.org/10.1109/TSP.2021.3088755>
- [15] Wu, Q., Zhang, R. (2019). Beamforming optimization for wireless network aided by intelligent reflecting surface with discrete phase shifts. *IEEE Transactions on Communications*, 68(3): 1838-1851. <https://doi.org/10.1109/TCOMM.2019.2958916>
- [16] Wang, P., Fang, J., Yuan, X., Chen, Z., Li, H. (2020). Intelligent reflecting surface-assisted millimeter wave communications: Joint active and passive precoding design. *IEEE Transactions on Vehicular Technology*, 69(12): 14960-14973. <https://doi.org/10.1109/TVT.2020.3031657>
- [17] Pan, C., Ren, H., Wang, K., Xu, W., Elkashlan, M., Nallanathan, A., Hanzo, L. (2020). Multicell MIMO communications relying on intelligent reflecting surfaces. *IEEE Transactions on Wireless Communications*, 19(8): 5218-5233. <https://doi.org/10.1109/TWC.2020.2990766>
- [18] Majid, A. (2021). Lifetime extension of three-dimensional wireless sensor networks, based on gaussian coverage probability. *Journal Européen des Systèmes Automatisés*, 54(4): 569-574. <https://doi.org/10.18280/jesa.540406>
- [19] Satrusallya, S., Mohanty, M.N. (2021). Design of antenna array for ku-Band Wireless Application. *Instrumentation, Mesures, Métrologies*, 20(2): 107-112.
- [20] Premkumar, M., Arun, M., Priya, S.S., Prathipa, R., Gurupandi, D. (2022). Physical (PHY) layer analysis of data transmission in MIMO wireless networks in Line-of-Sight (LoS) environments. *Mathematical Modelling of Engineering Problems*, 9(1): 210-214.
- [21] Zhao, Y.H., Jia, X.D., Cao, S.N. (2021). Energy efficiency optimization method for relay cooperative D2D communication. *Journal of Signal Processing*, 37(5): 854-861.
- [22] Chu, M.J., Qiu, R.H. (2021). Tradeoff Between Energy Efficiency and Spectrum Efficiency in Decode-and-Forward One-Way Multi-Relay Networks. *Computer Engineering*, 47(6): 182-187.
- [23] Majid, A. (2020). Reliability and failure rate evaluation of lifetime extension analysis of ad hoc and wireless sensor networks. *Mathematical Modelling of Engineering Problems*, 7(3): 411-420. <https://doi.org/10.18280/mmep.070311>
- [24] Liaskos, C., Nie, S., Tsioliaridou, A., Pitsillides, A., Ioannidis, S., Akyildiz, I. (2018). A new wireless communication paradigm through software-controlled metasurfaces. *IEEE Communications Magazine*, 56(9): 162-169. <https://doi.org/10.1109/MCOM.2018.1700659>
- [25] Kumar, S., Dixit, A.S. (2021). A miniaturized CSRR loaded 2-element MIMO antenna for LTE band. *Mathematical Modelling of Engineering Problems*, 8(6): 984-988.
- [26] Pandith, M.M., Ramaswamy, N.K., Srikantaswamy, M., Ramaswamy, R.K. (2022). A comprehensive review of geographic routing protocols in wireless sensor network. *Information Dynamics and Applications*, 1(1): 14-25. <https://doi.org/10.56578/ida010103>
- [27] Pakyürek, M., Dikmen, O., Kulaç, S. (2022). Exponentially-weighted based dynamic pilot power allocation in massive MIMO systems. *Traitement du Signal*, 39(2): 627-631. <https://doi.org/10.18280/ts.390225>